SEISMIC BEHAVIOUR OF TRIANGULAR ALLUVIAL VALLEYS SUBJECTED TO VERTICALLY PROPAGATING INCIDENT SV WAVES

Jafar NAJAFIZADEH
PhD Candidate of Geotechnical Engineering Research Center, IIEES, Tehran, Iran
j.najafizadeh@iiees.ac.ir

Peyman AMINPOUR
Graduate Student of Geotechnical Engineering Research Center, IIEES, Tehran, Iran
p.aminpour@iiees.ac.ir

Mohsen KAMALIAN
Associate Professor of Geotechnical Engineering Research Center, IIEES, Tehran, Iran
kamalian@iiees.ac.ir

Mohammad Kazem JAFARI
Professor of Geotechnical Engineering Research Center, IIEES, Tehran, Iran
jafari@iiees.ac.ir

Keywords: Triangular Alluvial Valleys, Amplification, Site Effects, Topography Effect, Spectral Finite Element, Wave Propagation

ABSTRACT

This paper is concerned with the problem of soil amplification and seismic site effects due to the local topographical and geotechnical characteristics. It focuses on 2D triangular alluvial valleys subjected to vertically propagating incident SV waves. The medium is assumed to have a linear elastic constitutive behaviour. All calculations are executed in time-domain using the spectral finite element method. Clear perspectives of the amplification patterns of the valley are presented by investigation of the frequency-domain responses. It is shown that the amplification pattern of the valley and its frequency characteristics depend strongly on its shape ratio. The maximum amplification ratio along the ground surface occurs at the center of the valley. A simple formula has been proposed for making initial estimation of the natural period of the valley in site effect microzonation studies. The natural frequency of the triangular alluvial valley decreases as the shape ratio of the valley decreases.

INTRODUCTION

It has long been recognized that site effects can significantly affect the nature of ground motion during earthquakes. Local conditions can generate large amplifications and important spatial variations of ground shaking. These effects are relevant in assessing seismic risk, in planning, in the seismic design of important facilities and in calculating the response of long structures. There is a close relation between earthquake damage and topographic and geological irregularities. There have been numerous cases of recorded motion and observed earthquake damage pointing towards topographic amplification as an important effect. Very high accelerations recorded at the Pacoima Dam (1.25 g) during the 1971 San Fernando Earthquake (Trifunac & Hudson, 1971; Boore, 1973) and at Tarzana Hill (1.78 g) during the 1994 Northridge Earthquake (Spudich et al., 1996) can be partly attributed to topographic effects. Thorough geophysical and geotechnical surveys, in combination with the utilization of small seismographic arrays and various analytical or numerical simulations, have suggested that the aforementioned discrepancy may be attributed to the existence of subsurface irregularities, like alluvial valleys or sedimentary basins (Aki and Larner, 1970; Aki, 1988 and 1993; Trifunac, 1971; Sanchez-Sesma and Esquivel, 1979; Bard and Bouchon, 1980; Sanchez-Sesma et al., 1988; Graves, 1996; Bao et al., 1996; Bard, 1997; Faccioli et al., 1997; Kokusho and Matsumoto, 1998; Bielak et al., 1999, Paolucci, 1999). It was realized that, apart from the soil- material conditions, the geomorphic features of a valley (in 2 dimensions) or a basin (in 3 dimensions) tend to alter and usually aggravate the amplitude, frequency content, duration, and spatial variability of ground shaking. The main phenomena that constitute the "valley amplification" effects on site response have been summarized for the geotechnical community by Aki (1988) and Finn (1991); some newer major seismic events have dramatically reinforced their main conclusions. A typical example of valley effects is the damage distribution observed during the 1988 Armenia earthquake. Yegian et al. (1994), trying to correlate the observed damage with the ground shaking in the city of Kirovakan, located about 10 to 15 km from the surface outbreak of the fault, pointed out that 1-D analyses substantially underestimated the ground surface motion in a region of Kirovakan in which the soil profile constitutes a small triangular-shaped alluvial valley; the observed damage was adequately explained by Bielak et al. (1999) who provided a satisfactory explanation performing two-dimensional (2-D) ground response analyses for the same valley. Numerical studies have also shown that the extent of damage reported in the Marina District, San Francisco, during the 1989 Loma Prieta earthquake, could be mainly attributed to the 2-D site conditions (Bardet et al., 1992; Graves, 1993; Zhang and Papageorgiou, 1996). Graves (1998), simulating the seismic response of the San Fernando basin in the 1994 Northridge earthquake, showed that the subsurface irregularities may have caused a large amplification, especially in the long period ground motions. Finally, during the 1995 Hyogoken-Nambu earthquake, most of the damage in the city of Kobe occurred within the so-called "disaster belt", a narrow zone 1 km wide, nearly 20 km long, located between about 1 to 1.5 kilometers from the Rokko mountain rock outcrop. Numerical analyses by various researchers (Kawase, 1996; Takemiya, 1996; Kokusho and Matsumoto, 1998; Pitarka et al., 1998; Matsushima and Kawase, 1998; Hisada et al., 1998) have supported the idea that the 2-D valley geometry (in combination with the unquestionable forward-rupture directivity effects) had led to that particular concentration of damage.

The above phenomena have been documented either by observations, or multi-dimensional site-specific ground response analyses (in 2 or 3 dimensions).

As mentioned above, the "entrapment" of seismic waves in the valley and the generation of surface waves at the edges of the valley are phenomena expected to have the following "valley amplification" effects:

- The intensity of the ground shaking may be amplified at certain location more than 1-D wave-theory predicts. We will use the term "valley amplification" to describe the additional amplification, above the corresponding amplification computed with 1-D analysis. Such aggravation may be observed not only on the amplitude of the ground shaking (in terms of peak ground acceleration or velocity), but on its spectral content as well.
- The spatial variability of the ground surface motion may be substantial, even for closely-spaced locations characterized by the same soil profile. The ensuing differential motions are usually of great interest on the seismic response of long structures such as bridges and pipelines.

The seismic behaviour of valleys has been studied by many authors, by means of the finite difference method (Ohtsuki & Harumi, 1983), the finite-element method (Bielak & Xu, 1999; Castellani et al., 1982), the boundary element method (Barros et al., 1995; Luco et al., 1990 & 1995; Sanchez-Sesma et al., 1978, 1982 & 1991; Vogt et al., 1988; Wong et al., 1975) and the discrete wavenumber method (Kawase et al., 1988). The newest work has published recently by Kamalian et al. (2014) presents an advanced formulation of the spectral finite element method (SFEM). The goal of this paper is to capture numerically "valley amplification" effects on triangular alluvial valley by SFEM which was presented by Kamalian and Najafizadeh (2014).

NUMERICAL FORMULATION

The numerical parametric study was executed using the time domain spectral finite element formulation for 2-D elastodynamics. The governing equation for an isotropic, homogeneous, small-displacement body with linear elastic behavior can be written as the equilibrium equations for an elastic bounded medium $\Omega \subset R_d$ subjected to an external body-force f_i:

$$\pm_{ij,j} + f_i = \text{°}\ddot{u}_i \quad , \quad i = 1,...,d \tag{1}$$

where $\ddot{u}_i = \partial^2 u_i / \partial t^2$ is the second derivative of displacement of the medium with respect to time; ρ , the mass density, and $\pm_{ij}$ denotes the stress tensor components. Weak formulation of the corresponding governing equation for an elastic, isotropic and homogeneous body can be obtained using the well-known weighted residual method (Brebbia & Dominguez, 1989) as

$$\int_{\Gamma} t_i \cdot ¢u_i \cdot d\Gamma - \int_{\Omega} \pm_{ij} \cdot ¢£_{ij} \cdot d\Omega + \int_{\Omega} F_i \cdot ¢u_i \cdot d\Omega - \int_{\Omega} \text{°} \cdot \ddot{u}_i \cdot ¢u_i \cdot d\Omega = 0 \tag{2}$$

A spectral element approximation of Eq. (2) and its solution were obtained by Kamalian and Najafizadeh (2014). Spectral finite element method (SFEM) was implemented in a general purpose two-dimensional nonlinear and linear code named as NASEM (Najafizadeh, 2014). Several examples including site response analysis of rectangular alluvial valleys and ridge sections subjected to incident P and SV waves were solved in order to show the accuracy and efficiency of this implemented SFEM algorithm in carrying out site response analysis of topographic structures (Kamalian & Najafizadeh, 2014).

In the Spectral Finite Element Method, control points $¶_p \quad p = 0,...,n_\ell$, needed in defining the equation (3) in Lagrange polynomials of degree n_l are placed at special positions called Legendre-Gauss-Lobatto (LGL) points. Place of the control points is determined through solving the (5) equations:

$$h_n^{n_l}(¶) = \frac{(¶ - ¶_1)(¶ - ¶_2)...(¶ - ¶_{n-1})(¶ - ¶_{n+1})...(¶ - ¶_{n_l+1})}{(¶_n - ¶_1)(¶_n - ¶_2)...(¶_n - ¶_{n-1})(¶_n - ¶_{n+1})...(¶_n - ¶_{n_l+1})} \tag{3}$$

$$-1 \le ¶ \le 1, \quad n = 1,......., n_l + 1 \tag{4}$$

$$(1 - ¶^2) * L'_{n_l}(¶) = 0 \quad , \quad (1 - ¦^2) * L'_{n_l}(¦) = 0 \tag{5}$$

where, L'_{n_l} is first derivative of Lagrange polynomials of degree n_l .

By using these control points, the computational errors decrease exponentially. This method can converge faster to the exact solution than FEM due to using fewer degrees of freedom with almost the same accuracy. Control points make the mass matrix diagonal, which saves time and memory efficiently. In the SFEM, integrations of the matrices may be approximated using the Legendre-Gauss-Lobatto (LGL) quadrature rule in integration over the elements Ω_e :

$$\int_{\Omega_e} f(\vec{x}) dxdy = \int_{-1}^{1}\int_{-1}^{1} f(\vec{x}(¶,¦)) J_e(¶,¦) d¶d¦ \approx \sum_{p,q=0}^{n_\ell} µ_p µ_q f_{pq} J_{e(pq)} \tag{6}$$

w_p, w_q are the weights associated with the LGL points of integration, and $J_{e(pq)} = J_e(¶_p, ¦_q)$.

A highly interesting property of the SFEM is the fact that the mass matrix [M] is diagonal due to using LGL quadrature for each element (Komatitsh et al., 1999). This allows for a very significant reduction in computational cost and complexity.

Figure 1 shows the geometry and discretization of a triangular alluvial valley subjected to vertically propagating incident SV wave of the Ricker type (Figure 2):

$$f(t) = A_{\max}[1 - 2(®f_p(t - t_0))^2] e^{-(®f_p(t - t_0))^2} \tag{7}$$

where f_p , t_0 and $A_{\max}$ denote the predominant frequency, the time shift parameter and the maximum amplitude of the displacement time history, which were chosen as 2.4 Hz, 0.9 s and0.0001 m, respectively.

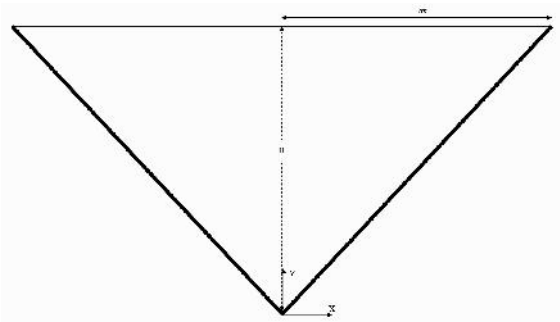

Figure1. Geometry of the 2-D homogenous triangular alluvial valley

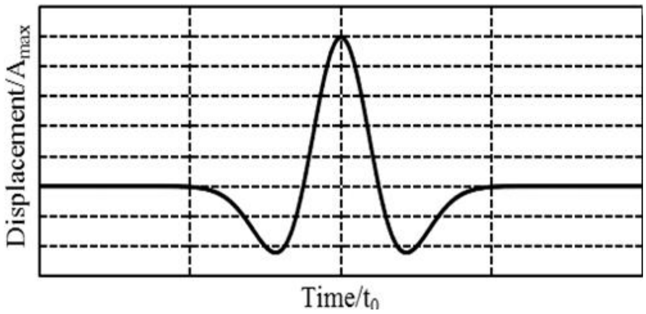

Figure 2. Displacement time history of the incident wave

METHODOLOGY OF PARAMETRIC ANALYSIS

The geometry of the 2-D homogenous triangular alluvial valley investigated by this study was defined in Fig. 1 where H and ax denote the thickness of center line and the half-width of the soil layer along the ground surface, respectively. The parametric study was mainly aimed to find out the answers of the following questions: What is the maximum amplification potential of the valley? Where does it occur along the valley? How does the amplification pattern vary along the valley? Does increasing the shape ratios (H/ax) of the valley necessarily mean intensifying the amplification potential at any point along it? Could extract a simple formula in order to get an initial estimation of the natural period of a rectangular alluvial valley could be useful in site effect microzonation studies?

In order to find out the answers of the above mentioned questions, the valley was subjected to the vertically propagating incident SV wave of the Ricker type (Figure 2), the thickness of the soil layer was selected as 50 m. The broad range of 2D triangular alluvial valleys resting on a rigid bed rock with different shape ratios (H/ax) of 0.2, 0.4, 0.6, 0.8, 1.0 and 2.0 encountered frequently in the nature were considered. The mechanical behavior of soil with values of Poisson's ratio as 0.33, damping ratio as 0.05, mass density as 2.0 t/m3 and shear wave velocity of the medium as 300 m/s were considered. As only the amplification curves along the surface of the valley was aimed to be studied, the same vertically propagating incident SV wave of the Ricker type (Figure 2) was subjected to the valley. Because altering the input motions would not affect the amplification pattern in a linear elastic media.

RESULTS OF PARAMETRIC ANALYSIS

This section presents the most important results obtained by the executed parametric study, which demonstrate the general amplification pattern of 2D triangular alluvial valleys resting on a rigid bed rock and show how it is affected by the shape ratio.

GENERAL AMPLIFICATION PATTERN

Figure 3 demonstrates clear perspectives of the amplification patterns of various nodes along the ground surface of 2-D triangular valleys via the different shape ratios subjected to a vertically propagating incident SV wave. As can be seen, the amplification pattern of the triangular alluvial valley and its frequency characteristics depend strongly on its shape ratio. In each triangular alluvial valley and irrespective of its shape ratio, the maximum amplification ratio at each node along the ground surface occurs at a characteristic frequency which is uniform along the ground surface. This characteristic frequency could be named as the natural frequency of the Triangular alluvial valley. The value of the natural frequency of the triangular alluvial valley decreases as the shape ratio decreases and tends towards the natural frequency of the corresponding 1D uniform soil layer over the bed rock (W = Vs/4H). Vice versa and as expected, the value of the natural frequency of the triangular alluvial valley increases as its shape ratio increases. It can also be seen that in each triangular alluvial valley and irrespective of its shape ratio, the maximum amplification ratio along the ground surface occurs at the center.

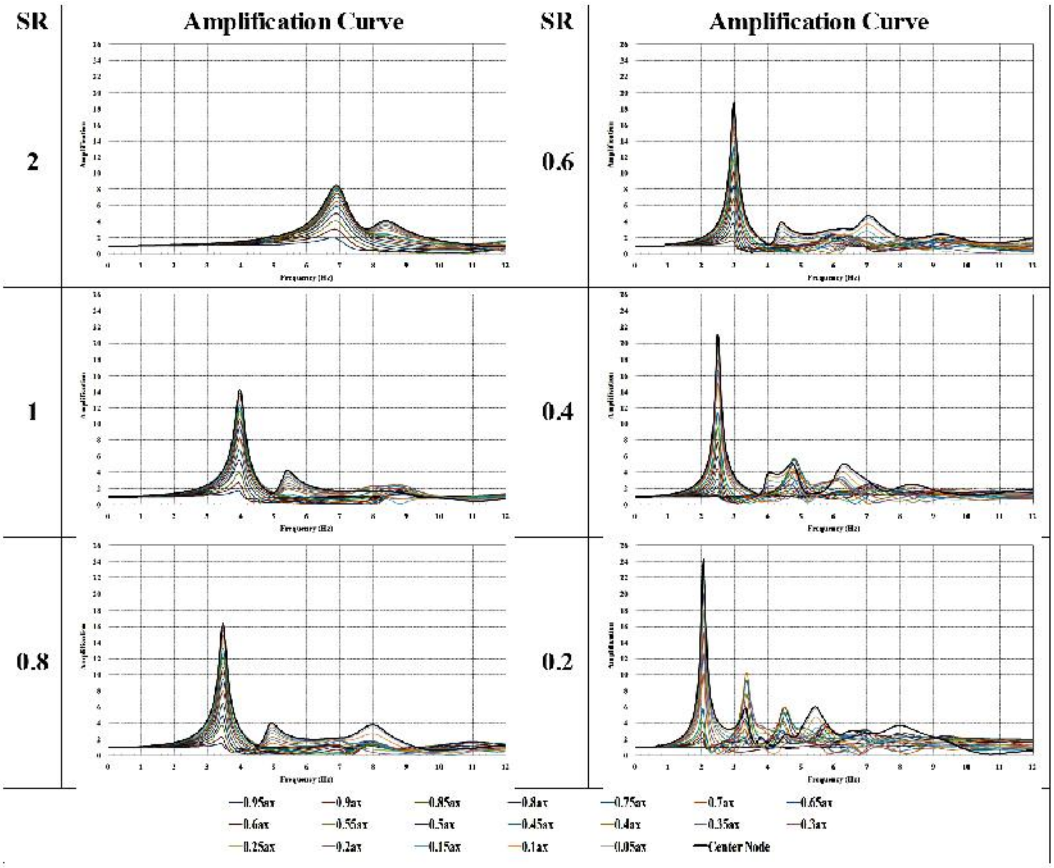

Figure 3. Comparison of the amplification curves of various nodes along the ground surface of triangular valley via the different shape ratios

MAXIMUM AMPLIFICATION

Figure 4 illustrates Changes of the maximum amplification of various nodes along the ground surface of triangular alluvial valley via the different shape ratios normalized to the maximum amplification of a 1D uniform homogeneous soil layer resting on a rigid bed rock (amplification ratio). As can be seen, it is confirmed that in each triangular alluvial valley and irrespective of its shape ratio, the maximum amplification ratio along the ground surface occurs at the center of the valley and when one moves from each of the corners towards the center, the maximum amplification ratio of the ground surface increases. No clear relation could be detected between the maximum amplification ratio and the shape ratio of the triangular alluvial valley. The amplification ratio of the triangular alluvial valley of the central point gets its maximum value at a shape ratio of 0.2 and decreases gradually as the shape ratio increases from 0.2 to 2.

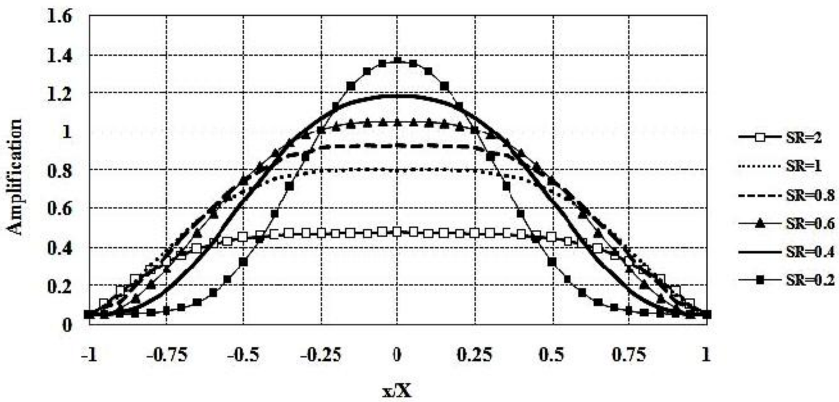

Figure 4. Comparison of the maximum amplification ratio change along the triangular alluvial valley via the different shape ratios

SHAPE RATIO EFFECT

Figure 5 compares the amplification curves of the center of the triangular alluvial valley with different shape ratios with the amplification curve of the corresponding 1D uniform homogeneous soil layer resting on a rigid bed rock. As can be seen, when the shape ratio decreases, the natural frequency of the triangular alluvial valley decreases and the amplification curve of the center node (2D case) moves towards the amplification curve of the corresponding 1D case. Although in all triangular alluvial valleys with shape ratio of less than 0.6, the maximum amplification ratio at the center node is more than that corresponding to the 1D case, but in the triangular alluvial valley with a shape ratio of more than 0.6 it's decreased.

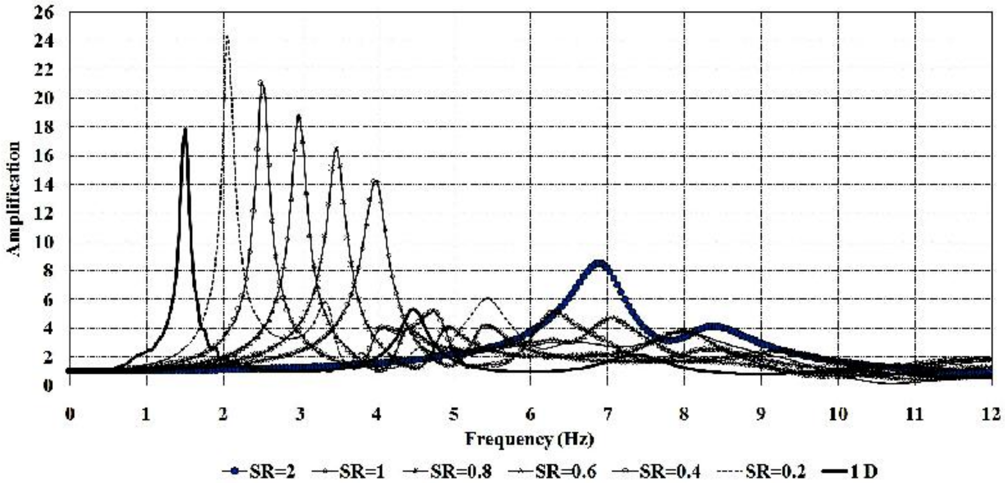

Figure 5. Amplification curves at top of the centerline of the triangular alluvial valley
(Vs = 300 m/s) with different shape ratios

NATURAL PERIOD OF A TRIANGULAR ALLUVIAL VALLEY

Extracting a simple formula in order to get an initial estimation of the natural period of a triangular alluvial valley could be useful in site effect microzonation studies. Fig.6 demonstrates how the natural frequency of the triangular alluvial valley alters with its shape ratio. Two curves are presented that corresponds to two different alluvials with a shear wave velocity of 300 and 400m/s, respectively. As can be seen, the curves are similar and infuse the idea of being capable to become non-dimensionalized. Fig.7 demonstrates these two curves once again, this time normalized to the natural frequency of the corresponding 1D uniform soil layer over the bed rock. As expected, the curves coincide and the ratio of the natural frequency of a triangular alluvial valley (F_{2D}) to the natural frequency of the corresponding 1D uniform soil layer over the bed rock (F_{1D}) can be approximated as a function of the shape ratio by the following formula:

$$F_{2D}/F_{1D} = 1.297 \cdot \exp(0.655 \cdot SR)$$

which can be re-written as:

$$F_{2D} = 1.297 \cdot \exp(0.655 \cdot SR) \cdot \left(V_s/(4 \cdot H)\right)$$

Where, Vs represents shear wave velocity, H triangular valley depth, and SR the valley shape ratio (SR=H/ax)

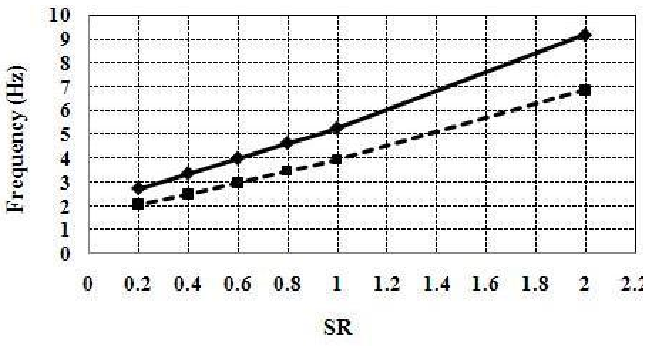

Figure 6. Natural frequency of the triangular alluvial valley via its shape ratio for two different shear wave velocities of 300 and 400 m/s

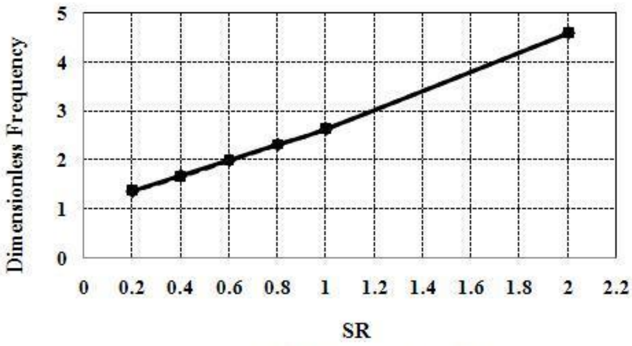

Figure 7. Dimensionless frequency of the triangular alluvial valley via its shape ratio

CONCLUSION

This paper focuses on 2D triangular alluvial valleys subjected to vertically propagating in-plane incident shear waves. All calculations are executed in time-domain using the spectral finite element method. A numerical parametric study was carried out on the seismic response of triangular alluvial valleys subjected to vertically propagating incident SV waves. It is shown that the amplification pattern of the triangular alluvial valley and its frequency characteristics depend strongly on its shape ratio. A natural frequency can be defined for the triangular alluvial valley so that at all nodes along the ground surface, the highest amplification factor occurs at this predominant frequency. The natural frequency of the triangular alluvial valley decreases towards the natural frequency of the corresponding 1D uniform soil layer on bed rock, as the shape ratio of the valley decreases. The maximum amplification ratio along the ground surface occurs at the center of the valley and decreases when one moves towards the corners. A simple formula has been proposed for initial estimation of the natural period of triangular alluvial valleys which can be used in site effect microzonation studies.

REFERENCES

Aki K (1988) Local site effects on strong ground motion, Earth- quake Engineering and Soil Dynamics II, ASCE

Aki K(1993) Local site effects on weak and strong ground motion, Tectonophysics, 218, 93-111

Bao H, Bielak J, Ghattas O, Kallivokas LF, O'Hallaron DR, Shewchuk J and Xu J (1996) Earthquake ground motion modeling on parallel computers, *Proc. ACM W IEEE Supercomputing Conference*, Pittsburgh, USA

Bard PY and Bouchon MA (1980) The seismic response of sediment filled valleys, Parts I-II, Bulletin of the Seismological Society of America, 70

Bielak J, Xu J and Ghattas O (1999) Earthquake ground motion and structural response in alluvial valleys, Journal of Geotechnical and Geoenvironmental Engineering, 125, 413-423

Boore DM (1973) The effect of simple topography on seismic waves: implications for the accelerations recorded at Pacoima Dam, San Fernando Valley, California, Bull. Seism. Soc. Am., 63, 1603–1609

Finn WDL (1991) Geotechnical engineering aspects of seismic microzonation, Proc. 4th International Conference on Seismic Zonation, Stanford, 1, 199-250

Graves RW (1993) Modeling three-dimensional site response effects in the Marina District Basin, San Francisco, California, Bulletin of the Seismological Society of America, 83, 1042-1063

Graves RW (1996) Simulating seismic wave propagation in 3-D elastic media using staggered grid finite differences, Bulletin of the Seismological Society of America, 86, 1091-1106

Kawase H (1988) Time-domain response of a semicircular canyon for incident SV, P and Rayleigh waves calculated by the discrete wavenumber boundary element method. Bull Seismol Soc Am, 78:1415–37

Kawase H (1996) The cause of the damage belt in Kobe: "The basin-edge effect", Constructive interference of the direct S-wave with the basin-induced diffracted Rayleigh waves, Seismological Research Letters, 67(5), 25-34

Komatitsch D and Tromp J (1999) Introduction to the spectral element method for three-dimensional seismic wave propagation, Geophys. J. Int., Vol. 139, 806-822

Matsushima S and Kawase H (1998) 3-D wave propagation analysis in Kobe referring to "The basin-edge effect", 2nd International Symposium on the Effects of Surface Geology on Seismic Motion, Yokohama, III, 1377-1384

Najafizadeh J, Kamalian M, Jafari MK and Khaji N (2014) Seismic Analysis of Rectangular Alluvial Valleys Subjected to Incident Sv Waves by Using the Spectral Finite Element Method. International Journal of Civil Engineering (IJCE) (ISI)

Sáanchez-Sesma FJ and Esquivel JA (1979) Ground motion on alluvial valleys under incident plane SH waves, Bulletin of the Seismological Society of America, 69, 1107-1120

Sáanchez-Sesma FJ, Chavez-Garcia F and Bravo MA (1988) Seismic response of a class of alluvial valley for incident SH waves, Bulletin of the Seismological Society of America, 78(1), 83-95

Spudich P, Hellweg M and Lee WHK (1996) Directional topographic site response at Tarzana observed in aftershocks of the 1994 Northridge, California, Earthquake: implications for main shock motions, Bull. Seism. Soc. Am., 86, S139–S208

Trifunac MD (1971) Surface motion of a semi-cylindrical alluvial valley for incident plane SH waves, Bulletin of the Seismological Society of America, 61, 1755-1770

Vogt RF, Wolf JP and Bachmann H (1988) Wave scattering by a canyon of arbitrary shape in a layered half-space, Earthquake Eng Struct Dyn, 16:803–12

Wong H and Jennings P (1975) Effect of canyon topographies on strong ground motion, Bull Seismol Soc Am, 65:1239–57

Yegian MK, Ghahraman VG and Gazetas G (1994) Seismological, soil and valley effects in Kirovakan, 1988 Armenia earthquake, Journal of Geotechnical Engineering, ASCE, 120(2), 349-365